

Bayesian structural damage detection of steel towers using measured modal parameters

Heung-Fai Lam^a and Jiahua Yang*

*Department of Architecture and Civil Engineering, City University of Hong Kong,
Tat Chee Avenue, Kowloon, Hong Kong*

(Received April 4, 2014, Revised August 8, 2014, Accepted September 18, 2014)

Abstract. Structural Health Monitoring (SHM) of steel towers has become a hot research topic. From the literature, it is impractical and impossible to develop a “general” method that can detect all kinds of damages for all types of structures. A practical method should make use of the characteristics of the type of structures and the kind of damages. This paper reports a feasibility study on the use of measured modal parameters for the detection of damaged braces of tower structures following the Bayesian probabilistic approach. A substructure-based structural model-updating scheme, which groups different parts of the target structure systematically and is specially designed for tower structures, is developed to identify the stiffness distributions of the target structure under the undamaged and possibly damaged conditions. By comparing the identified stiffness distributions, the damage locations and the corresponding damage extents can be detected. By following the Bayesian theory, the probability model of the uncertain parameters is derived. The most probable model of the steel tower can be obtained by maximizing the probability density function (PDF) of the model parameters. Experimental case studies were employed to verify the proposed method. The contributions of this paper are not only on the proposal of the substructure-based Bayesian model updating method but also on the verification of the proposed methodology through measured data from a scale model of transmission tower under laboratory conditions.

Keywords: Bayesian approach; damage detection; steel tower; modal identification; model updating

1. Introduction

Structural Health Monitoring (SHM) becomes more and more important. Many countries, such as China and Australia, are trying to include SHM in their design codes. Structural damage detection is an important component in SHM. Many damage detection methods have been developed to monitor the health status of structures; they can be divided into two categories: local approach (also called non-destructive evaluation) and global approach. The local approach includes traditional techniques, such as visual inspection, dye penetrant methods and ultrasonic techniques (Burdekin 1993, Popovics and Rose 1994). The global approach includes mainly the dynamic methods, such as the non-model based methods (Kim *et al.* 1992, Yang *et al.* 2004) and

*Corresponding author, Ph.D. Student, E-mail: oldsky007@gmail.com

^aAssociate Professor, E-mail: paullam@cityu.edu.hk

model-based methods (Lam *et al.* 2004, Lam *et al.* 2008). The proposed method in this paper follows the global approach utilizing the vibration measurements of the target structure under the undamaged (reference) and possibly damaged status. The dynamic responses of the target structure are measured and modal parameters, such as natural frequencies and mode shapes, are identified. Next, the modal parameters identified from the undamaged and possibly damaged structures are used to update the structure models separately. The two updated models are compared to identify the existence, location and extent of the damage. Although the traditional local approach has been well developed, the relatively new dynamic methods are attracting more and more attention. This is because the local approach requires the direct accessibility of the investigation locations and the preliminary knowledge of the damage locations. Furthermore, the equipment involved in the local approach is usually expensive and the operations are time consuming. Unlike the local approach, the dynamic methods can identify damage in a global sense without prior information about the locations of damage. Moreover, with the advances in measurement technologies, dynamic responses of structures can be measured accurately and economically. Although the dynamic damage detection methods have many superior aspects, there are challenges, which have to be addressed through intensive research. Model updating is an inverse problem, and uncertainties due to incomplete measurement and modeling error make this inverse problem non-unique (sometimes even ill-posed). This paper addresses the problem of uncertainty by following the Bayesian probabilistic approach, which was first developed by Beck and Katafygiotis in references (Beck and Katafygiotis 1998, Katafygiotis and Beck 1998).

Transmission towers, as a kind of steel towers, play a significant role in people's daily life. For this type of structures, the buckling of secondary members (braces) due to strong wind during typhoon is common. If the buckled braces are not detected and repaired, the accumulation of damage may lead to collapse of the tower and result in unimaginable loss. For example, Hundreds of transmission towers bulked during the ice storm in Canada 1998 (Magix 2008). Over 4 million people in Canada and parts of the US lose power supply in the middle of winter for over three weeks. Multiple deaths were reported, and many from hypothermia. From the accident report, it was found that the braces of these collapsed transmission towers were seriously damaged, but the foundations were basically undamaged. On 14 December 2011, another tragedy happened in Sichuan, China. A transmission tower collapsed when 13 labors was doing daily maintenance work, killing 8 and injuring 3 (ChinaFotoPress/Getty Images AsiaPac 2011). Many other transmission tower damage related disasters were reported worldwide. These incidents clearly show the importance of structural damage detection of steel towers.

Damage detection of large-scale three-dimensional structures, like steel towers, is a difficult task. Apart from the difficulties in extracting reliable modal parameters and establishing an accurate computer model, the large number of structural members is an essential problem. Even with modern computer technology, it is time consuming to consider the stiffness values of all members individually in the model updating process. Despite the computational efficiency, the uncertainties associated with the large number of identified model parameters will be extremely high if the amount of measurement cannot be increased accordingly. This is because the information that can be extracted from the measurement is limited. Therefore, an appropriate substructure scheme to group members together so as to reduce the number of uncertain model parameters is critical for the success of structural damage detection in large-scale structures. Although many vibration-based damage detection methods were developed, due to the above mentioned difficulties, they were verified using simple structures and computer simulations like two-dimensional trusses (Li and Law 2010), beams (Zhong and Oyadiji 2011), and shear buildings

(Lam and Ng 2008). It is unclear if these methods are applicable for large-scale and three-dimensional structures. One of the contributions of this paper is the verification of the proposed method by a scale model of a three-dimensional transmission tower with hundreds of DOFs.

Lam and co-workers proposed to integrate the dynamic condensation method and structural model updating in developing a damage detection method for transmission towers (Yin *et al.* 2009, Lam and Yin 2011). After condensation, the transmission tower was parameterized as a multistory building with one uncertain parameter per story. As a result, only the damaged story can be detected. Furthermore, the modeling error of the condensed structure is relatively large that affect the accuracy of the damage detection results. This paper presents a method that is different from the one in reference (Yin *et al.* 2009, Lam and Yin 2011) for the damage detection of braces of steel towers by integrating a substructure scheme with the Bayesian model updating method.

A scale model of steel tower was built in the Structural Vibration Laboratory (SVL) of City University of Hong Kong (see Fig. 1). Impact hammer tests were carried out, and the natural frequencies and mode shapes of the steel tower were identified. Model updating was conducted by following Bayesian model updating approach (Vanik *et al.* 2000). The superior aspect of the Bayesian model updating approach is that all information in the measured data can be fully utilized, while many methods usually use only the mean values (or the most probable values) of measured modal parameters. It must be pointed out that the Bayesian model updating approach focuses not only on the most probable values (MPV) of model parameters but also the corresponding reliability by calculating the posterior PDF of uncertain model parameters conditional on the selected class of models and the set of measured data. This is essential for decision making in practice.

In the experimental verification, different damage patterns were considered by removing brace members at different locations. For each damage pattern, the modal parameters of the “damaged” tower were identified utilizing vibration data from impact hammer tests. Bayesian model updating was conducted to identify the “optimal” model of the structure in each damage pattern. “Damage” is defined as the reduction in stiffness of the braces, or equivalently, a reduction in braces’ modulus of elasticity. The damage can then be identified by comparing the model updating results based on the measurements from the “undamaged” and “damaged” tower. The experimental verification results are very encouraging showing that structural damage detection of steel towers based on Bayesian model updating is feasible.

2. Proposed methodology

The proposed structural damage detection methodology consists of three main components. These are the modal identification, the substructure-based model updating, and structural damage detection utilizing the model updating results. The MODE-ID method (Beck 1978) is adopted for modal identification in this study. Owing to the limited space in this paper, the formulation of the MODE-ID method is not repeated here. In the following subsections, the details of the Bayesian model updating, the proposed substructure scheme and structural damage detection methodology are presented.

2.1 Bayesian model updating

The original formulation of the Bayesian statistical system identification framework (Beck and

Katafygiotis 1998) was developed using measured time domain data. It was extended to use measured modal parameters in reference (Vanik *et al.* 2000). For a complicated structure like the transmission tower, model updating in time domain is extremely difficult. This paper focuses on the application of the Bayesian model updating method (Vanik *et al.* 2000) utilizing measured modal parameters.

Instead of pinpointing a set of model parameters in the deterministic approach, the Bayesian approach aims in calculating the posterior PDF of the uncertain model parameters conditional on a selected class of models and a given set of measurements (Beck and Katafygiotis 1998)

$$p(\boldsymbol{\theta}|\mathbf{D}, S) = cp(\boldsymbol{\theta}|S)p(\mathbf{D}|\boldsymbol{\theta}, S) \tag{1}$$

where $\boldsymbol{\theta}$ is the vector of uncertain model parameters to be identified; \mathbf{D} represents the set of measured data and it is the measured modal parameters in this study; S represents the selected model class (including both the class of deterministic structural models and the class of probabilistic models for describing the uncertainty associated with the prediction error); c is a normalizing constant such that the integration of the posterior PDF over the parameter space equals to unity; $p(\boldsymbol{\theta}|S)$ is a prior PDF allowing the subjective judgment from engineers or researchers to be incorporated in the model updating process. A uniform prior PDF can be used to let the measured data control the results of model updating. The essential part in Eq. (1) is the likelihood function $p(\mathbf{D}|\boldsymbol{\theta}, S)$. In an impact hammer test, a set of modal parameters can be identified per impulse. In practice, many impulses can be applied separately. Therefore, many sets of modal parameters can be measured. It is assumed that the measured modal parameters in different data sets are independent. Furthermore, the independence is also assumed among different modes as well as between natural frequency and mode shape (Yaglom 1987, Yuen *et al.* 2002). As a result, Eq. (1) can be expressed as

$$p(\boldsymbol{\theta}|\mathbf{D}_n, S) = c_0 \prod_{i=1}^{N_m} \prod_{n=1}^{N_s} p(\hat{\omega}_{i,n}^2 | \boldsymbol{\theta}, S) p(\hat{\boldsymbol{\phi}}_{i,n} | \boldsymbol{\theta}, S) \tag{2}$$

where \mathbf{D}_n represents the n^{th} set of data, which consists of measured modal parameters of the first N_m modes. N_s is the number of data sets (i.e., the number of impulses considered). $\hat{\omega}_{i,n}^2$ and $\hat{\boldsymbol{\phi}}_{i,n}$ are the squared circular natural frequency (i.e., eigenvalue in (rad/s)²) and mode shape of the i^{th} mode identified from the n^{th} set of data, respectively; c_0 is a constant which absorbed the normalizing constant c and the uniform prior PDF. The formulation of PDF for natural frequency and mode shape (i.e., $p(\hat{\omega}_{i,n}^2 | \boldsymbol{\theta}, S)$ and $p(\hat{\boldsymbol{\phi}}_{i,n} | \boldsymbol{\theta}, S)$) are given in reference (Vanik *et al.* 2000) and are not repeated here. By substituting these two expressions into Eq. (2) one obtains the posterior PDF of the uncertain parameters as follows

$$\begin{aligned} p(\boldsymbol{\theta}|\mathbf{D}, S) &= c_1 \prod_{i=1}^{N_m} \prod_{n=1}^{N_s} \exp \left(-\frac{1}{2} \left(\frac{(\hat{\omega}_{i,n}^2 - \omega_i^2(\boldsymbol{\theta}))^2}{\varepsilon_i^2} + \frac{\boldsymbol{\psi}_i(\boldsymbol{\theta})^T (\mathbf{I} - \hat{\boldsymbol{\phi}}_{i,n} \hat{\boldsymbol{\phi}}_{i,n}^T) \boldsymbol{\psi}_i(\boldsymbol{\theta})}{\sigma_i^2 \|\boldsymbol{\psi}_i(\boldsymbol{\theta})\|^2} \right) \right) \\ &= c_1 \exp \left(-\frac{1}{2} \sum_{i=1}^{N_m} \sum_{n=1}^{N_s} \left(\frac{(\hat{\omega}_{i,n}^2 - \omega_i^2(\boldsymbol{\theta}))^2}{\varepsilon_i^2} + \frac{\boldsymbol{\psi}_i(\boldsymbol{\theta})^T (\mathbf{I} - \hat{\boldsymbol{\phi}}_{i,n} \hat{\boldsymbol{\phi}}_{i,n}^T) \boldsymbol{\psi}_i(\boldsymbol{\theta})}{\sigma_i^2 \|\boldsymbol{\psi}_i(\boldsymbol{\theta})\|^2} \right) \right) \end{aligned} \tag{3}$$

In Eq. (3), $\omega_i^2(\boldsymbol{\theta})$ and $\boldsymbol{\psi}_i(\boldsymbol{\theta})$ are the calculated squared circular natural frequency and mode shape of the i^{th} mode, respectively. Their dependence on the uncertain parameter $\boldsymbol{\theta}$ is emphasized.

The superscript “ T ” represents the transpose of a matrix. ε_i^2 is the sample variance of the squared circular natural frequency. It can be calculated using the identified natural frequencies from different data sets. Similarly, σ_i^2 is the variance of the mode shape, and it can be calculated as (Vanik *et al.* 2000)

$$\sigma_i^2 = \frac{1}{N_s} \sum_{n=1}^{N_s} \frac{\|\hat{\Phi}_{i,n} - \bar{\Phi}_i\|^2}{\|\hat{\Phi}_{i,n}\|^2} \tag{4}$$

$\|\cdot\|$ represents the Euclidean norm. $\bar{\Phi}_i$ is the sample mean of the mode shape of the i^{th} mode. \mathbf{I} is the identity matrix. Note that all mode shapes are normalized to have unit Euclidean norm. The measure-of-fit function (i.e., the objective function) $J(\boldsymbol{\theta})$ is defined as

$$J(\boldsymbol{\theta}) = \sum_{i=1}^{N_m} \sum_{n=1}^{N_s} \left(\frac{(\hat{\omega}_{i,n}^2 - \omega_i^2(\boldsymbol{\theta}))^2}{\varepsilon_i^2} + \frac{\boldsymbol{\Psi}_i(\boldsymbol{\theta})^T (\mathbf{I} - \hat{\Phi}_{i,n} \hat{\Phi}_{i,n}^T) \boldsymbol{\Psi}_i(\boldsymbol{\theta})}{\sigma_i^2 \|\boldsymbol{\Psi}_i(\boldsymbol{\theta})\|^2} \right) \tag{5}$$

To obtain the most probable parameter vector $\boldsymbol{\theta}^*$ one needs to maximize the PDF of uncertain parameters in Eq. (3). It is equivalent to minimize the objective function $J(\boldsymbol{\theta})$ in Eq. (5). Under the deterministic approach, only the mean values are considered and a lot of information in the measured data is in fact sacrificed. In the Bayesian probabilistic approach, one can see in Eq. (5) that the terms with the subscript n represent the individual measured data set. All the measured data are fully utilized to make the statistical inference. The factors $1/\varepsilon_i^2$ and $1/\sigma_i^2$ in Eq. (5) can be treated as the “weighting factors” in model updating. It is clear that the weighting factor for a measured quantity will be become large if the corresponding variance (i.e., uncertainty) is low. This is a well-known characteristic of the Bayesian approach. The objective function $J(\boldsymbol{\theta})$ is implicit, and the numerical minimization of $J(\boldsymbol{\theta})$ is conducted by the active-set algorithm for obtaining the most probable model parameter vector $\boldsymbol{\theta}^*$, which is considered as the optimal model based on the sets of measurement, \mathbf{D}_n .

2.2 Damage detection

In order to do damage detection, the optimal model of the undamaged structure is first identified, which is used as a reference (or baseline). Usually the number of members of a tower is large and the information that can be extracted from the measurement is limited. If one assigns one uncertain parameter to each member, the updated model parameters will be unreliable. Therefore, the parameterization according to the type of damages to be detected and the characteristics of the target structure is crucial. This is the main reason why it is difficult to develop a “general” method for detecting all kinds of damages for all kinds of structures. A substructure scheme was proposed to organize the structural members in potential damaged groups. A theoretically rigorous substructure method for Bayesian model updating can be found in reference (Papadimitriou *et al.* 2013). By considering only brace damages of steel towers, the proposed damage detection procedures are summarized as follows:

- (1) To estimate the nominal values of material properties: The Young’s modulus of steel and aluminum (the braces are made of aluminum), and the mass of steel plates at joints (small steel plates are welded at joints to work as gusset plates for connecting the braces) need to be estimated. Model updating is carried out with the uncertain parameter vector $\boldsymbol{\theta}_a = [\theta_m, \theta_{Es}, \theta_{Ea}]$, where $\theta_m, \theta_{Es},$

and θ_{Ea} scale the plate mass, Young's modulus of steel, and Young's modulus of aluminum, respectively, by minimizing Eq. (5) using data from the undamaged structure.

(2) To identify the reference system: According to experience, the lower part of a transmission tower is usually easier to be damaged by wind load than the upper part. It is proposed that only the lower five levels of the tower (see Fig. 2) are considered for damage detection. Using the symmetrical property of the tower, only two uncertain stiffness parameters are used for each level (see Fig. 2 for the definition of levels). One scales the Young's modulus of braces on faces perpendicular to the x -axis (Faces A and C), and the other is for the braces on faces perpendicular to y -axis (Faces B and D). Altogether, there are ten uncertain parameters in the model updating process. The uncertain parameter vector is defined as

$$\boldsymbol{\theta}_{ud} = [\theta_{1AC}, \theta_{1BD}, \theta_{2AC}, \theta_{2BD}, \theta_{3AC}, \theta_{3BD}, \theta_{4AC}, \theta_{4BD}, \theta_{5AC}, \theta_{5BD}] \quad (6)$$

The subscript “ ud ” represents that this vector is for the undamaged structure. The subscript “ $1AC$ ” consists of two parts. The first digit shows the level number and the two letters represents the faces. Therefore, θ_{1AC} represents the stiffness factor for braces on Faces A and C at the first level. Based on the nominal values estimated in step 1, model updating is conducted for identifying the parameter vector in Eq. (6) based on the measured data of the undamaged structure. The optimal model identified in this step is treated as the reference model.

(3) To update the possibly damaged structure: The data measured from the possibly damaged structure are used to do model updating (minimize the objective function in Eq. (5)) with the same model class as the reference model. Finally, the stiffness distributions of the undamaged (reference) and possibly damaged structures are compared, and damage can be detected at the positions of stiffness reduction.

3. Experimental verification

3.1 Experimental setup

Fig. 1 shows the scale model of a transmission tower, which consists of 8 levels, and 4 types of members: (1) the four columns, (2) beams, (3) cross arm members, and (4) braces. The columns, beams and cross arm members are made of steel, and all braces are made of aluminum. The columns, beams and cross arm members are connected by welding. Small steel plates are welded to all beam-column joints for the installation of braces through bolted connections. There are four faces named Faces A, B, C and D at each level. For example, nodes 2-3-12-11 enclose Face A of level 2, and nodes 11-12-30-29 enclose Face B of level 2 (see Fig. 2). Face A of level 2 is highlighted by dash line in Fig. 2 to show the definition of face.

In real application of structural damage detection, it is difficult to distribute sensors throughout the entire structure. To simulate this situation, sensors were installed only on one column for measuring vibrations in x and y directions. The instrumented column is the one with nodes 1 to 9 as shown in Fig. 2. Since only 9 sensors were available, the measurement was divided into two setups. They are measurements along the x and y direction, respectively, and a reference sensor was installed at node 9 at an angle of 45° between the positive x and y directions (see Fig. 3). This reference sensor can pick up the vibration in both x and y directions. As a result, even one setup focused on vibration along x direction and the other focused on vibration along y direction, the



Fig. 1 Scale model of transmission tower

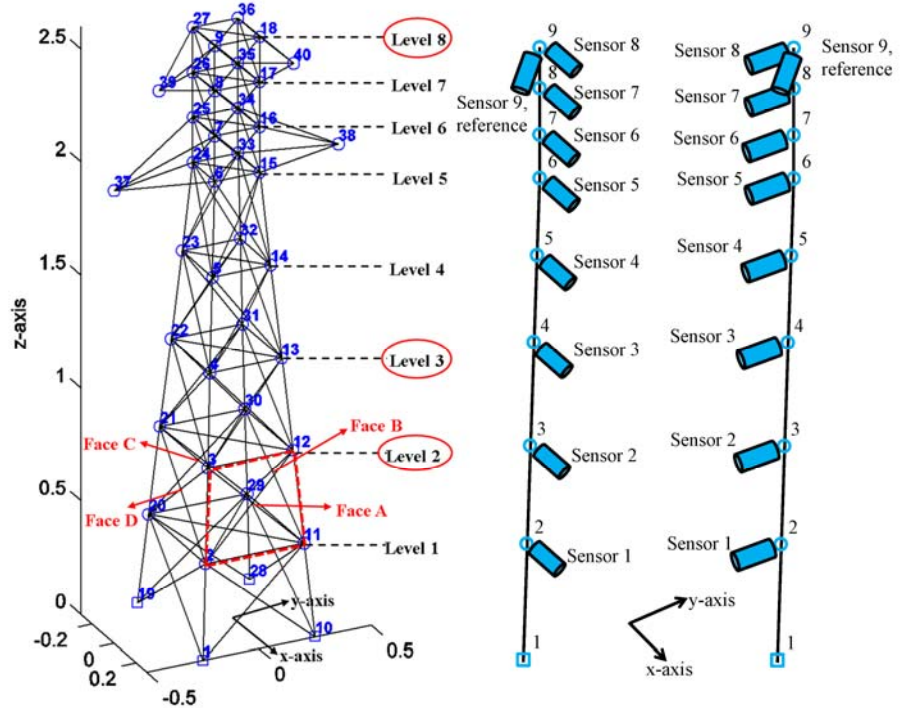


Fig. 2 Finite element model of the steel tower

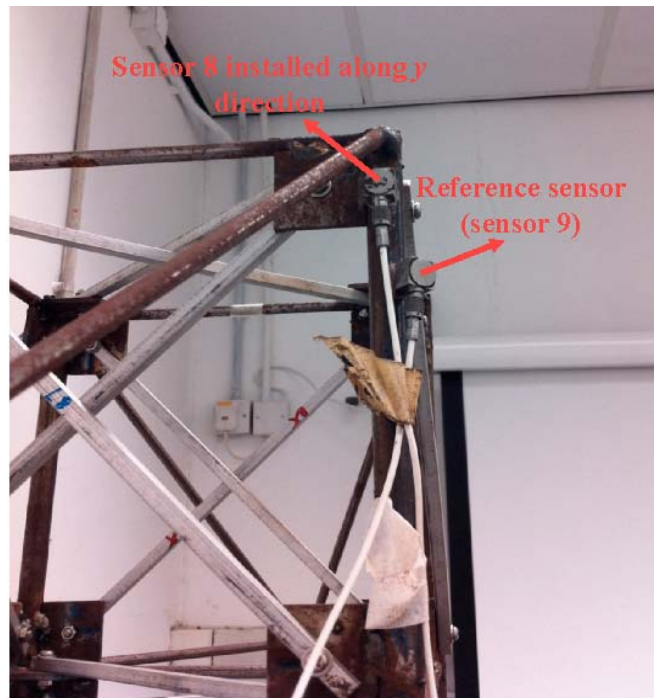


Fig. 3 Directions of sensors in setup 2

reference sensor can help in identifying modes with vibration in both directions, such as the torsional modes, and assembling mode shapes from the two setups. The configurations of the sensors of the two setups are shown in detail in the middle and right parts of Fig. 2. In the first setup, eight sensors were installed at nodes 2 to 9 along the x direction. The eight sensors were connected to channels 1 to 8 of the NI-9234 module with channel 9 as the reference sensor. The impact excitation was individually applied many times at levels 2, 3 and 8 along the x direction (see the circled levels in Fig. 2). In the second setup, the eight sensors were installed at nodes 2 to 9 along the y direction. The impact excitations were applied in a similar manner as in the first setup but along the y direction. The arrows in Fig. 3 show the positive directions of sensors.

3.2 Impact hammer test and modal identification

The modal parameters of measured responses along the x direction are identified first. Fig. 4 shows the acceleration response at channel 1 when the steel tower was excited by impact hammer along x direction (measurement from other sensors are similar). The responses in all channels were cut into segments according to the impulses as illustrated in Fig. 4. Each segment of responses can be treated as a free vibration response. In this way multiple data sets were obtained (each data set corresponding to one impulse). The cross-spectral of all channels (with channel 9 as the reference) were calculated. Fig. 5 shows the average cross-spectrum (average over all segments, all excitation locations in all channels) for vibration along x direction. The frequencies at the peaks are indicated in the average spectrum for reference. Those frequencies are employed as initial trials for modal identification of each segment of measured data using the MODE-ID method.

For vibration along x direction, there are 62 segments of data in total. Each segment of data, which consists of responses from 9 sensors, was analyzed one by one using MODE-ID. Multiple sets of identified modal parameters are available for model updating. The mean values (average over all segments of data) of identified natural frequencies for vibration along x direction are shown in Table 1 (modes 2, 3 and 5). The variances of the squared circular natural frequencies are also shown. The larger the value of variance, the higher the uncertainty associated with the identified modal parameters will be. Fig. 6 shows the identified mode shapes along x direction. The lines with circle markers represent the undeformed shapes of the measured column. The dash lines with triangular markers represent the upper and lower bounds of the identified mode shapes. It means that all the mode shapes identified from different segments of time domain data vary within the area between the two dash lines. The solid lines with triangular marker represent the average mode shapes. From Fig. 6, the second mode shape varies in a wider range than the other two modes showing that the uncertainty of the second mode shape is larger than the other two. The upper and lower bounds of the first mode shape almost overlap, which indicates that the first mode shape is very certain. The “sample variances” of mode shapes along x direction calculated by Eq. (4) are also shown in Table 1 (modes 2, 3 and 5). In Bayesian model updating, the objective function $J(\theta)$ in Eq. (5) is minimized with appropriate weighting factors determined from the variances in Table 1.

Following a similar procedure, experiments were conducted for vibration along y direction. Due to the limited space, the average spectrum and the identified mode shapes for vibration along y direction are not presented here. The average natural frequencies for vibration along y direction together with the variances are shown in Table 1 (modes 1, 3 and 4). It must be pointed out that the second mode along x and y directions belong to the same mode, which is a torsional mode (i.e., mode 3 in Table 1). Finally, five modes were identified. They are two x -translational modes (the

2nd and 5th modes), two *y*-translational modes (1st and 4th modes) and one torsional mode (the 3rd). These five modes were employed in the model updating process for the purpose of damage detection.

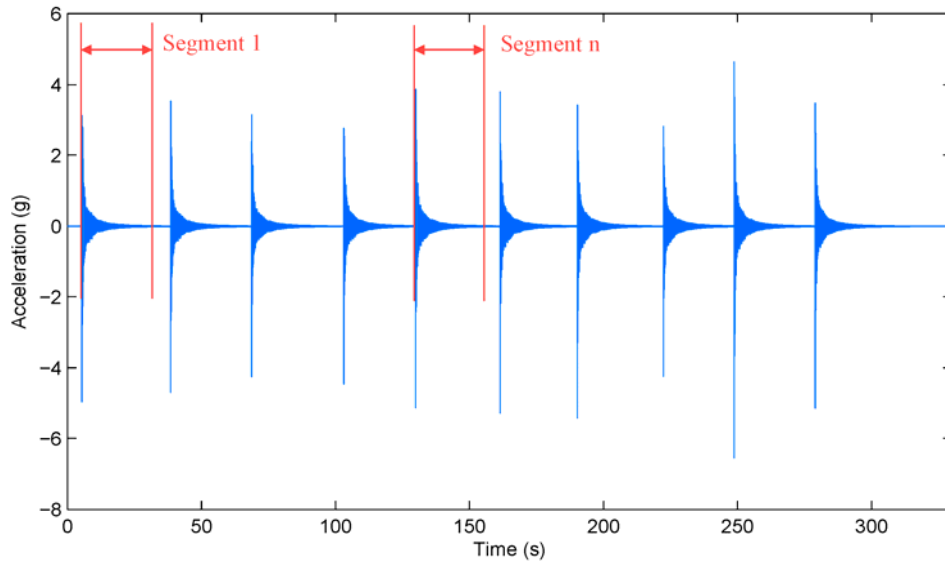


Fig. 4 Typical measured time-domain response under impact excitation

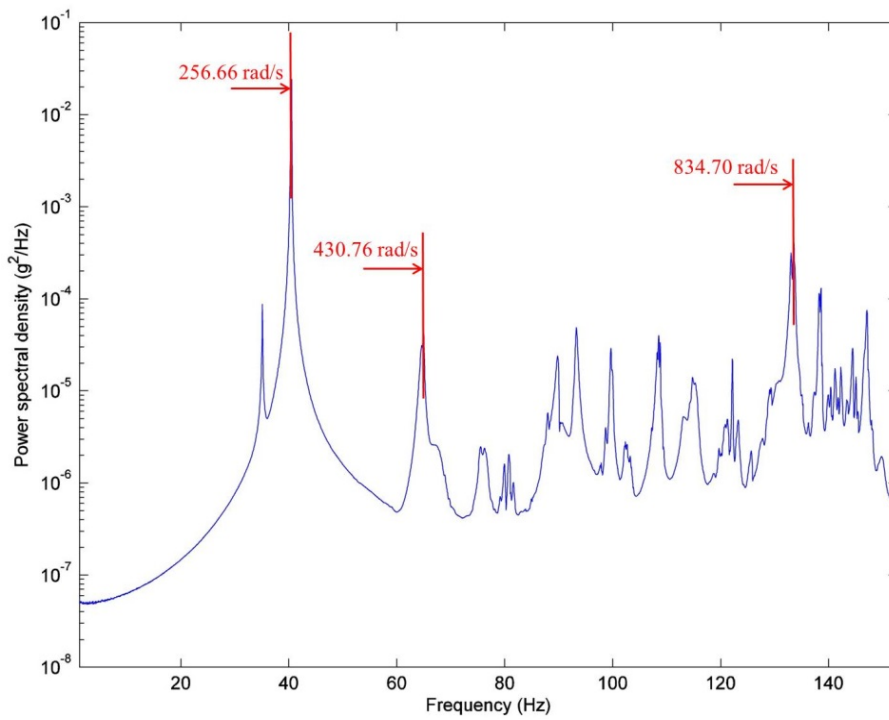


Fig. 5 The average spectrum for vibration along *x* direction

Table 1 Measured average natural frequencies (ω) of undamaged tower together with the sample variances

	Mode 1	Mode 2	Mode 3		Mode 4	Mode 5
	1 st translational along y	1 st translational along x	Torsional		2 nd translational along y	2 nd translational along x
			x	y		
ω (rad/s)	222.23	256.03	425.74	428.69	578.22	836.77
Variance of ω^2 ((rad/s) ⁴)	4.221×10^2	5.008×10^3	2.417×10^7	4.565×10^6	3.494×10^7	1.703×10^7
Variance of mode shape	2.298×10^{-7}	4.684×10^{-7}	2.192×10^{-2}	3.837×10^{-3}	1.339×10^{-2}	2.610×10^{-3}

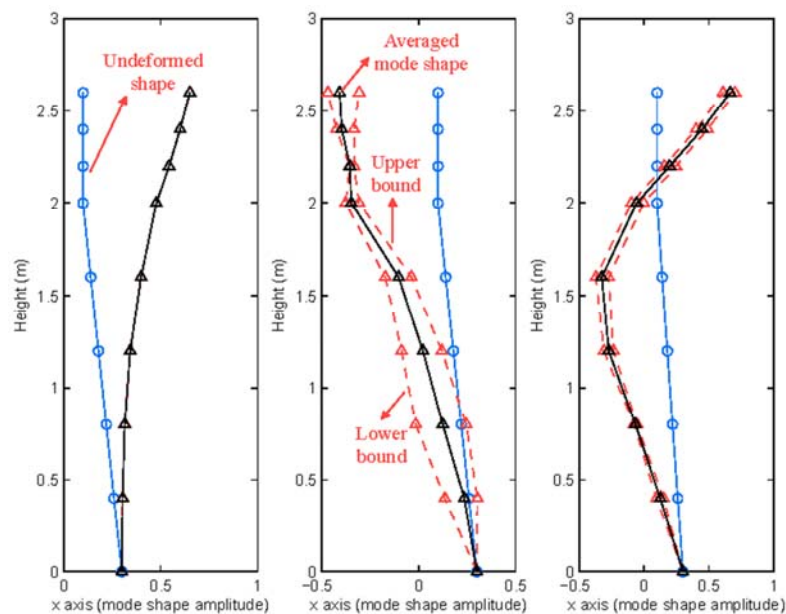


Fig. 6 Identified mode shapes along x direction

3.3 Bayesian model updating results

3.3.1 Undamaged structure

A self-developed finite element (FE) code is used to establish a three-dimensional FE model of the steel tower based on the matrix stiffness method (Kassimali 2011). Fig. 7 shows the three-dimensional mode shapes calculated by the self-developed FE program before model updating. The calculated mode shapes corresponding to the measured DOFs can be extracted from the three-dimensional mode shapes. With the measured and calculated modal parameters, one can update the computer model by following the Bayesian approach as presented in section 2.1 and obtain an optimal model to represent the structure.

The initial guesses of the mass of the steel plates at the joints, the Young's modulus of steel and aluminium are 21.06 g, 200 GPa and 69 GPa, respectively. To estimate a more reliable nominal values for these three model parameters, model updating was conducted by minimizing Eq. (5) with respect to uncertain parameter vector $\theta_a = [\theta_m, \theta_{Es}, \theta_{Ea}]$ (as discussed in section 2.2). All the

identified modal parameters from all data sets were employed in calculating the objective function value in Eq. (5). The most probable vector $\theta_a^*=[3.2018,1.1918,0.7616]$. It must be pointed out that those updated values are not the “true” values of plate mass and Young’s modulus of steel and aluminum. They are the “equivalent” values after the consideration of measurement noise and modeling error. For example, the updated value of Young’s modulus of steel is about 1.2. It doesn’t mean that the “true” value of Young’s modulus of the steel used in this tower is 20% higher than the standard value of 200GPa. It is just the “equivalent” value of Young’s modulus under the assumed class of models. One of the sources of modeling error is the rigid-joint assumption at the two ends of the braces. The natural frequencies of the updated model are compared to the measured ones (average) in Table 2. The small differences between the measured and model-predicted natural frequencies show that the result of model updating is acceptable. The optimal scaling factors in θ_a^* are multiplied to the initial values of the mass of the steel plate, Young’s modulus of steel and aluminium, respectively, to obtain the nominal values.

To obtain the reference system for damage detection, Bayesian model updating is conducted utilizing the data from the undamaged structure using the 10-parameter model class as given in Eq. (6). The optimal vector θ_{ud}^* is shown in Table 3. The identified stiffness factors are in general close to unity except for the stiffness for braces on Faces B and D at level 1. This may be caused by the workmanship issue during the construction of the tower. The comparisons of calculated and average measured modal parameters are summarized in Table 4 and Fig. 8, respectively. The first and second rows of Fig. 8 correspond to mode shapes along x and y directions, respectively. Each column of Fig. 8 corresponds to an individual mode. Noted that mode 3 is a torsional mode with

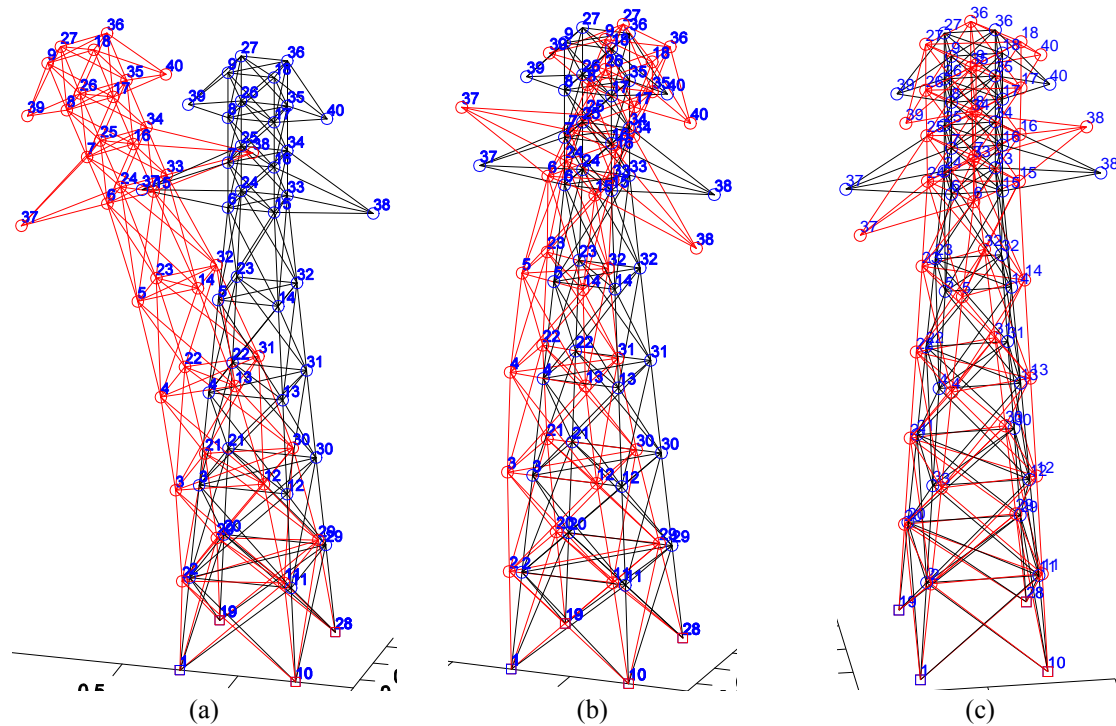


Fig. 7 Calculated mode shapes: (a) first translational mode along y , (b) second translational mode along y , (c) first torsional mode

Table 2 Comparison of the calculated and average natural frequencies of the undamaged tower for θ_a^*

	Mode 1	Mode 2	Mode 3	Mode 4	Mode 5
Measured (rad/s)	222.25	256.04	426.86	578.12	836.98
Calculated (rad/s)	222.01	257.88	401.48	642.94	831.75
% Difference	-0.11%	0.72%	-5.94%	11.21%	-0.63%

Table 3 The optimal vector θ_{ud}^* (the identified brace stiffness distribution in the undamaged case)

θ_{1AC}^*	θ_{1BD}^*	θ_{2AC}^*	θ_{2BD}^*	θ_{3AC}^*	θ_{3BD}^*	θ_{4AC}^*	θ_{4BD}^*	θ_{5AC}^*	θ_{5BD}^*
0.9651	0.5376	0.9484	0.9655	1.1701	1.2256	1.0394	1.0332	1.2292	1.1077

Table 4 Comparison of the calculated and average natural frequencies of the undamaged tower for θ_{ud}^*

	Mode 1	Mode 2	Mode 3	Mode 4	Mode 5
Measured (rad/s)	222.25	256.04	426.86	578.12	836.98
Calculated (rad/s)	222.30	256.27	408.97	635.32	831.12
% Difference	0.02%	0.09%	-4.19%	9.89%	-0.70%

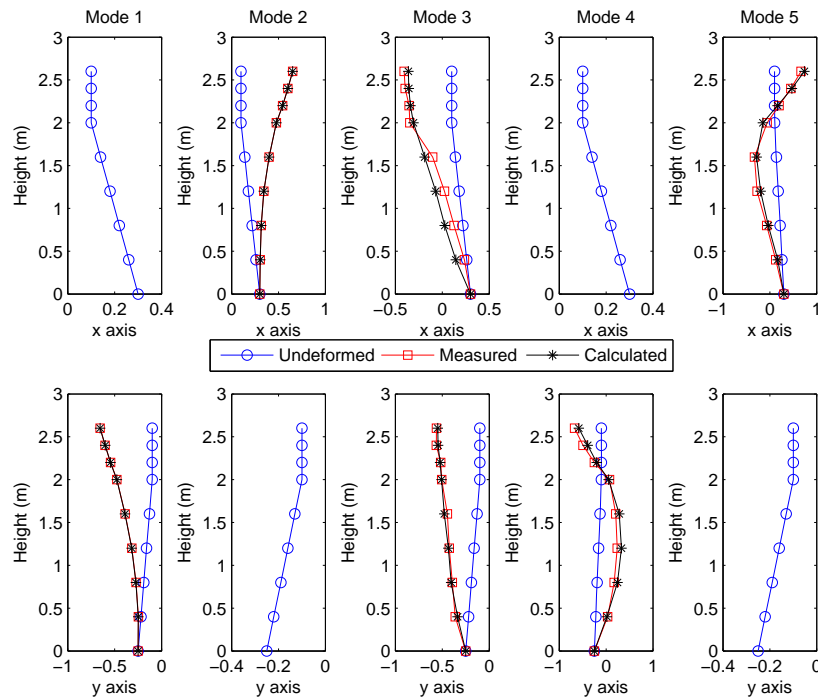


Fig. 8 Comparison of the calculated and average measured mode shapes of the undamaged tower for θ_{ud}^*

components in both x and y directions. Other modes are translational modes with only x or y component but not both. The matching is basically very good. From Table 4, it is observed that the percentage differences for modes 3 and 4 are larger than the others. This can be explained by the relatively large variances for natural frequencies in modes 3 and 4 (see Table 1). Since the

measured natural frequencies in these two modes are less certain, the Bayesian model updating assigned smaller weighting factors to these two modes. As a result, the system automatically spends less effort in matching these two natural frequencies. The identified optimal parameter factors of the undamaged structure (in Table 3) are multiplied to corresponding brace stiffness in the class of finite element model. The modified model class will be used to update the damaged structure. As a result, a parameter factor of value 1 represents no damage on the brace, and a value of say 0.6 represents a 40% reduction in brace stiffness.

3.3.2 Damage case 1

One brace on Face A at level 2 and one on Face D at level 4 are removed in this damage case (see Fig. 9). Modal identification was carried out for measured time-domain data from the damaged tower. The first five modes were identified, and Table 5 summarizes the mean values of identified natural frequencies averaged over all segments of data. The variances of the squared circular natural frequencies are shown in the table. Two natural frequency variances are available for mode 3. This is because mode 3 is a torsional mode and it was measured by two setups: one for vibration along x and the other for vibration along y . The comparison of the average natural frequencies for the damaged and undamaged tower is given in Table 5. The damage reduces the natural frequencies showing a reduction in stiffness in the damaged structure. The average mode shapes are shown Fig. 10. The “variances” of measured mode shapes are also given in Table 5.

By using the measured modal parameters of the damaged structure, Bayesian model updating is conducted using the 10-parameter model class. The vector of uncertain model parameters is denoted by $\theta_{d1}=[\theta_{1AC}, \theta_{1BD}, \theta_{2AC}, \theta_{2BD}, \theta_{3AC}, \theta_{3BD}, \theta_{4AC}, \theta_{4BD}, \theta_{5AC}, \theta_{5BD}]$. Note that the arrangement of θ_{d1} is exactly the same as that of θ_{ud} . The only difference is the subscript “d1”, which represents damage case 1.

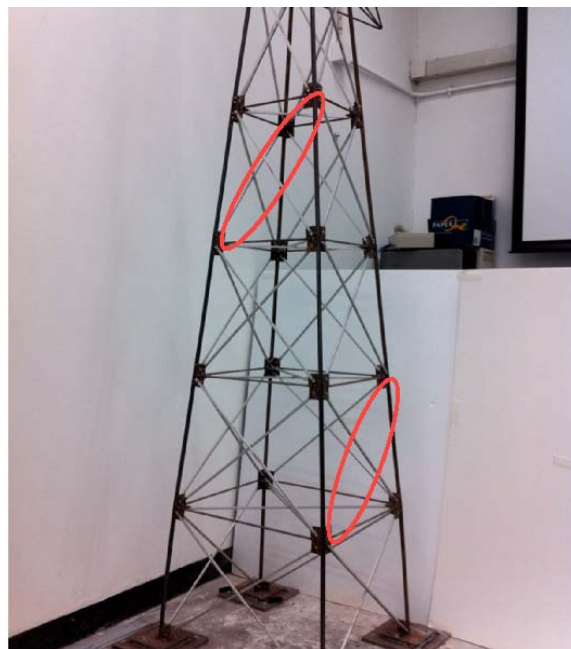


Fig. 9 Description of damage case 1

Table 5 Average measured natural frequencies (ω) of damage case 1 together with the sample variances

	Mode 1	Mode 2	Mode 3	Mode 4	Mode 5	
ω (damaged) (rad/s)	220.80	254.57	407.17	566.63	837.08	
ω (undamaged) (rad/s)	222.25	256.04	426.86	578.12	836.98	
% Difference	-0.65%	-0.57%	-4.61%	-1.99%	0.01%	
Variance of ω^2 ((rad/s) ⁴)	1.057×10^3	1.405×10^4	2.530×10^6	9.392×10^5	5.323×10^7	3.120×10^7
Variance of mode shape	3.088×10^{-7}	1.297×10^{-6}	5.597×10^{-3}	9.404×10^{-4}	5.117×10^{-2}	4.875×10^{-3}

Table 6 Comparison of calculated and average natural frequencies of damaged case 1

	Mode 1	Mode 2	Mode 3	Mode 4	Mode 5
Measured (rad/s)	220.80	254.57	407.17	566.63	837.08
Calculated (rad/s)	220.90	255.21	402.64	605.53	827.12
% Difference	0.04%	0.25%	-1.11%	6.87%	-1.19%

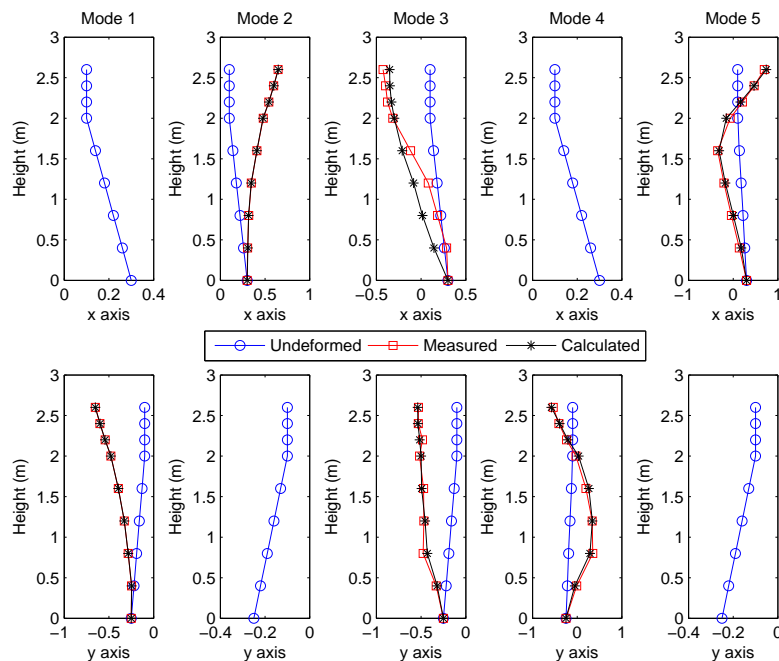


Fig. 10 Comparison of calculated and average measured mode shapes of damaged case 1

All the measured data sets were employed to minimize the objective function in Eq. (5). After model updating, the matching between the measured and calculated modal parameters is shown in Table 6 and Fig. 10. They match well indicating that the 10-parameter model class for detecting this type of damages is good. Based on the model updating result, the reductions in stiffness for all substructures are summarized in Fig. 11. It is obvious that the stiffness values for substructures 2AC and 4BD are reduced. This is consistent with the actual damage simulated on the structure.

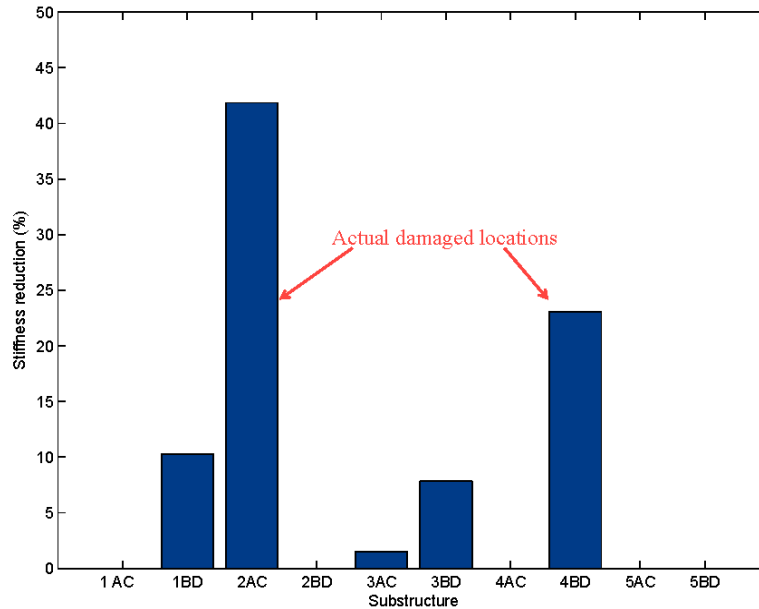


Fig. 11 Damage detection result of damage case 1

Small stiffness reduction can be observed for substructures 1BD, 3AC and 3BD, but their values are relatively small.

3.3.3 Damage case 2

In damage case 2, a large damage is introduced by removing both braces on Face D at level 4 (see Fig. 12). The experiment was carried out and the average measured natural frequencies were obtained and summarized in Table 7. The measured mode shapes are shown together with the calculated ones in Fig. 13. Table 7 also shows the variances of the measured natural frequencies and mode shapes. Compared to the undamaged tower, it can be observed that the damage induces large changes in the natural frequency and mode shape of the 3rd mode. Bayesian model updating is conducted with the vector of uncertain model parameters $\theta_{d2} = [\theta_{1AC}, \theta_{1BD}, \theta_{2AC}, \theta_{2BD}, \theta_{3AC}, \theta_{3BD}, \theta_{4AC}, \theta_{4BD}, \theta_{5AC}, \theta_{5BD}]$. The subscript “d2” represents damage case 2. The stiffness reductions in all substructures are calculated and summarized in Fig. 14. It is very clear that the stiffness reduction for substructure 4BD is the largest and very outstanding. This is consistent with the damage simulated on the structure in this damage case. It can be concluded that the proposed method successfully detects the damage in this case.

Apart from the substructure 4BD, the reductions in stiffness for substructures 1AC and 3BD are not small. This error may be caused by the employed sub-structure scheme, in which a single factor is employed to scale the brace stiffness on two parallel faces of a given level. The advantage of this sub-structure scheme is to reduce the number of uncertain model parameters in model updating. However, the trade-off is the introduction of large modelling error when the brace stiffness values on the two faces are very different. This is the situation in Damage case 2. When the two braces on Face D are removed, the brace stiffness on this face is dropped to almost zero while the brace stiffness on the opposite face (i.e., Face B) is 100%. Under such situation, the modelling error of the 10-parameter model class is not small.



Fig. 12 Description of damage case 2

Table 7 Average measured natural frequencies (ω) of damage case 2 together with the sample variances

	Mode 1	Mode 2	Mode 3	Mode 4	Mode 5	
ω (damaged) (rad/s)	222.04	247.29	383.85	574.14	833.17	
ω (undamaged) (rad/s)	222.25	256.04	426.86	578.12	836.98	
% Difference	-0.09%	-3.42%	-10.08%	-0.69%	-0.46%	
Variance of ω^2 ((rad/s) ⁴)	2.224×10^3	2.420×10^3	6.558×10^4	1.653×10^5	1.799×10^6	8.445×10^7
Variance of mode shape	1.353×10^{-7}	3.476×10^{-6}	1.380×10^{-3}	2.926×10^{-3}	2.396×10^{-3}	2.145×10^{-3}

Table 8 Comparison of calculated and average measured natural frequencies of damage case 2

	Mode 1	Mode 2	Mode 3	Mode 4	Mode 5
Measured (rad/s)	222.04	247.29	383.85	574.14	833.17
Calculated (rad/s)	221.65	247.10	383.58	609.64	799.02
% Difference	-0.17%	-0.07%	-0.07%	6.18%	-4.10%

To check if the class of models employed in model updating is appropriate, the average measured modal parameters and the modal parameters calculated by the optimal model are summarized in Table 8 and Fig. 13. The matching of natural frequencies is as good as that of natural frequencies in damage case 1. However, the matching of mode shape of mode 3 along the x direction is no good. It is not difficult to observe that the mode shape is only fitted in an “average” sense. Although there is limitation in the selected class of models, it is doing a reasonable job for both fitting the measurement and damage detection.

One possible way to improve the model class is to increase the number of uncertain parameters (i.e., increase the complexity of the model class). For example, one can increase the two parameters per level to four parameters per level. Then, the class of models can capture the

individual variation in brace stiffness on the four faces of a given level. In fact, this more complicated model class was employed, and the fitting between the measured and calculated mode shapes is very good including mode 3 (the results are not presented in this paper, owing to the limited space). However, the additional uncertain parameters require additional measurement to identify their values in acceptable accuracy. If no additional measurement is available, the uncertainties of the identified model parameters will become very large. Under such situation, the results of damage detection become very bad.

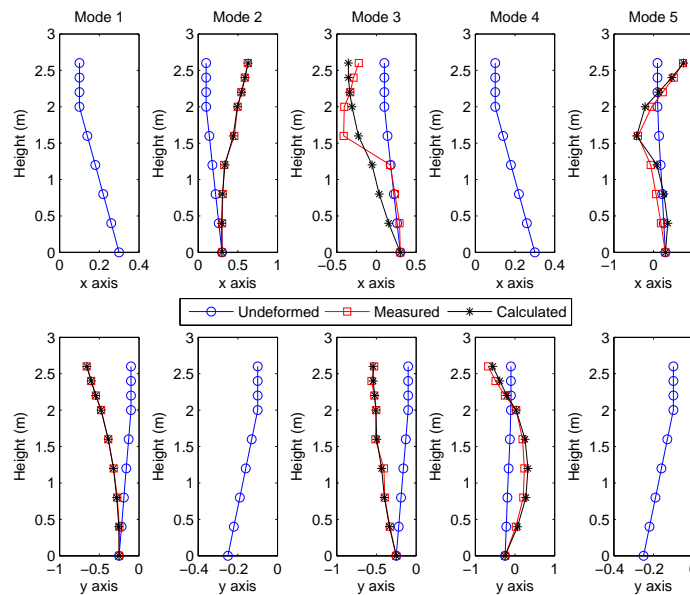


Fig. 13 Comparison of calculated and average measured mode shapes of damage case 2

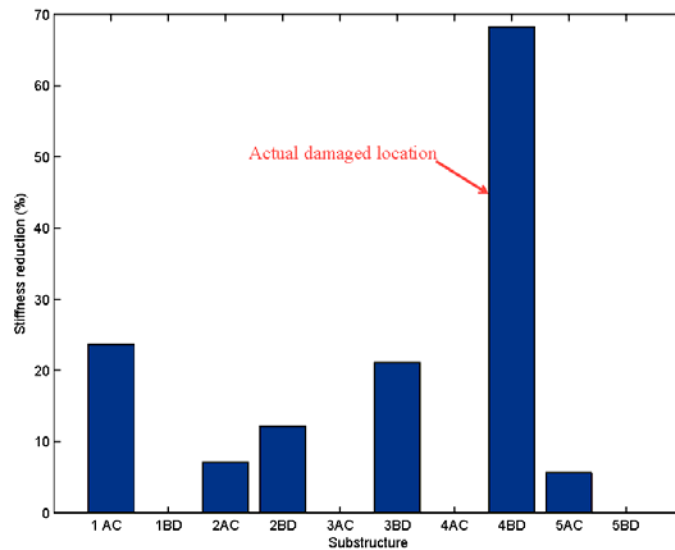


Fig. 14 Damage detection result of damage case 2

3.4 Comparison with damage vector method

The conventional damage vector method (Zimmerman and Kaouk 1994) was selected to do the damage detection of Damage case 1 again for comparison purpose. The most important formulations of the damage vector method are summarized here for the completeness of this paper. Considering the equation of motion of an n -DOF finite element model gives

$$\mathbf{M}\ddot{\mathbf{x}} + \mathbf{C}\dot{\mathbf{x}} + \mathbf{K}\mathbf{x} = \mathbf{0} \quad (7)$$

where \mathbf{M} , \mathbf{C} and \mathbf{K} are the n by n mass, damping and stiffness matrices, respectively. The eigenvalue problem of Eq. (7) can be expressed as

$$\left(\lambda_{hi}^2 \mathbf{M} + \lambda_{hi} \mathbf{C} + \mathbf{K}\right) \boldsymbol{\varphi}_{hi} = \mathbf{0} \quad (8)$$

where λ_{hi} and $\boldsymbol{\varphi}_{hi}$ are the i^{th} eigenvalue and eigenvector of the healthy structure, respectively (the subscript h denotes ‘‘healthy’’). The eigenvalue problem of the damaged structure can be obtained based on Eq. (8) as

$$\left(\lambda_{di}^2 (\mathbf{M} - \Delta\mathbf{M}) + \lambda_{di} (\mathbf{C} - \Delta\mathbf{C}) + (\mathbf{K} - \Delta\mathbf{K})\right) \boldsymbol{\varphi}_{di} = \mathbf{0} \quad (9)$$

where the subscript d denotes damaged; $\Delta\mathbf{M}$, $\Delta\mathbf{C}$ and $\Delta\mathbf{K}$ are the perturbation mass, damping and stiffness matrices due to structural damage, respectively. A damage vector \mathbf{d}_i for the i^{th} mode is defined by grouping the perturbation matrices on the right-hand side of Eq. (9)

$$\begin{aligned} \mathbf{d}_i &= \mathbf{Z}_{di} \boldsymbol{\varphi}_{di} \\ &= \left(\lambda_{di}^2 \Delta\mathbf{M} + \lambda_{di} \Delta\mathbf{C} + \Delta\mathbf{K}\right) \boldsymbol{\varphi}_{di} \end{aligned} \quad (10)$$

where the matrix \mathbf{Z}_{di} is obtained as follows

$$\mathbf{Z}_{di} = \lambda_{di}^2 \mathbf{M} + \lambda_{di} \mathbf{C} + \mathbf{K} \quad (11)$$

Two observations are obtained from Eq. (10) and Eq. (11). Firstly, if the j^{th} DOF of the structure is not directly affected by the damage, the j^{th} rows of the perturbation matrices will be zero. As a consequence, the j^{th} component of \mathbf{d}_i will be zero. In other words, \mathbf{d}_i can be used as the damage indicator, whose j^{th} nonzero component indicates that the j^{th} DOF of the structure is directly affected by the damage. Secondly, the damage vector \mathbf{d}_i can be determined based on the healthy structure (the original mass, damping and stiffness matrices) and the measured eigenvalues and eigenvectors of the damaged structure. The computation for the perturbation matrices is thus unnecessary. Eq. (10) gives the j^{th} component of \mathbf{d}_i

$$\mathbf{d}_i(j) = \mathbf{Z}_{di}(j,:) \boldsymbol{\varphi}_{di} = \left\| \mathbf{Z}_{di}(j,:) \right\| \left\| \boldsymbol{\varphi}_{di} \right\| \cos \theta_i^j \quad (12)$$

where $\mathbf{Z}_{di}(j,:)$ denotes the j^{th} row of the matrix \mathbf{Z}_{di} and θ_i^j is the angle between the vectors $\mathbf{Z}_{di}(j,:)$ and $\boldsymbol{\varphi}_{di}$. Note from Eq. (12) that if $\mathbf{d}_i(j)$ equals to zero, θ_i^j will equal to 90° , and if $\mathbf{d}_i(j)$ is different from zero, θ_i^j will not equal to 90° . Therefore, the difference between θ_i^j and 90° (denoted by α_i^j) can be used to locate damage

$$\alpha_i^j = \theta_i^j \left(\frac{180^\circ}{\pi} \right) - 90^\circ \quad (13)$$

If α_i^j is dramatically different from zero, the corresponding DOF is considered to be damaged. By applying Eq. (13) for each DOF the damage can be located. The above discussion assumes that only one mode is available. In practice, usually multiple modes are measured. The multi-mode version of Eq. (13) is given as follows (Zimmerman and Kaouk 1994)

$$\alpha^j = \frac{1}{M} \sum_{i=1}^M |\alpha_i^j| \tag{14}$$

where M is the number of measured modes. The procedures of damage vector method are summarized as follows:

1. Establish the finite element model of the target structure and calculate the matrix \mathbf{Z}_{di} for each mode by using Eq. (11). Note that the measured natural frequencies of the possibly damaged structure will be used for calculating the eigenvalues in Eq. (11).
2. Expand the measured mode shapes of the possibly damaged structure such that the DOFs of the measured mode shapes are consistent with the DOFs of the finite element model. The system equivalent reduction expansion process (O’Callahan *et al.* 1989) is adopted in this study.

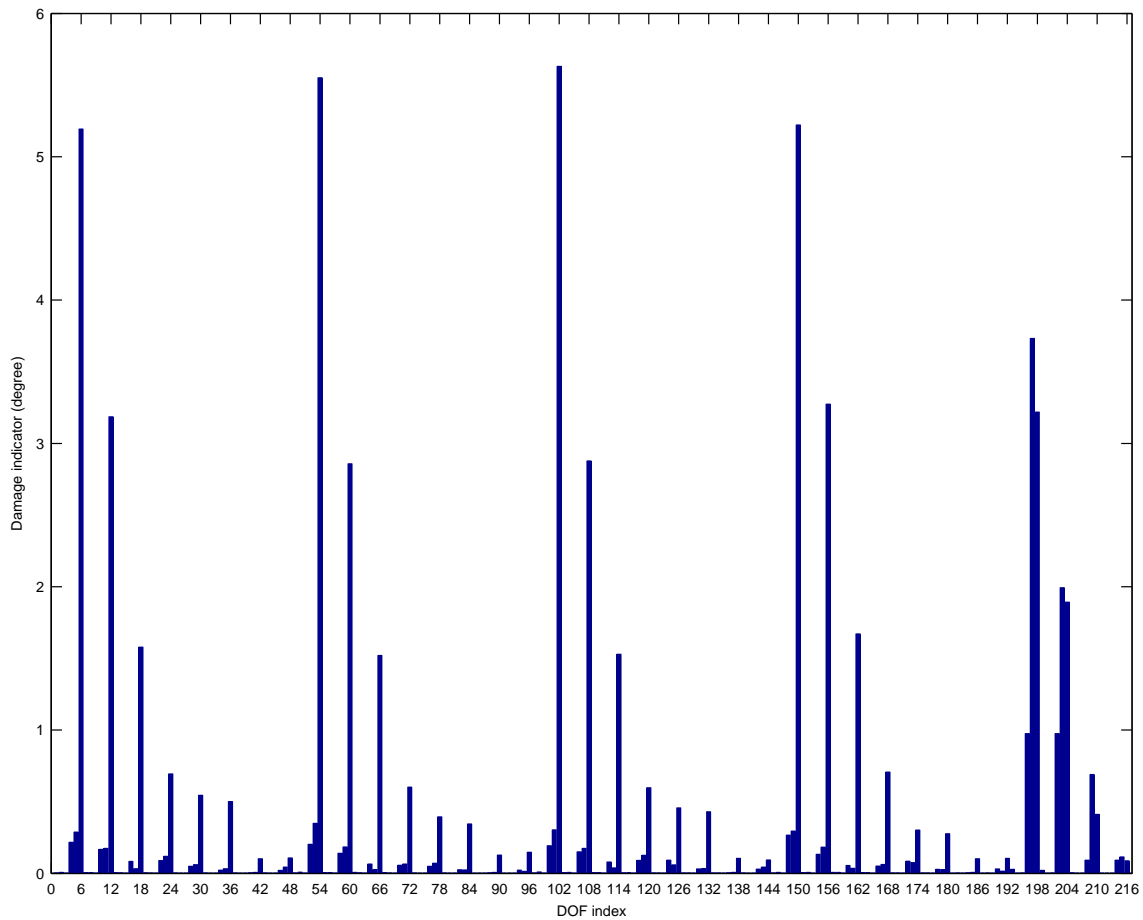


Fig. 15 Damage indicators of the transmission tower for damage case 1

3. Calculate the damage indicators of each DOF based on Eq. (14) using all the measured modes.

By following the damage vector method, the damage indicators for Damage case 1 were calculated and are presented in Fig. 15. It is clear from Fig. 15 that the damage indicators for DOFs 6, 12, 18, 24, 30, 36, 54, 60, 66, 72, 102, 108, 114, 120, 126, 132, 150, 156, 162, 168, 198, 204 and 210 are relatively large. They are corresponding to nodes 2 to 7, nodes 11 to 14, nodes 20 to 25, nodes 29 to 32 and nodes 37 to 39 (see Fig. 2 for the node numbering system. There are 6 DOFs at each node except the 4 support nodes. The numbering of the DOFs follows the order of the nodes). In Damage case 1, only two braces were damaged and the corresponding nodes are 2, 12, 22 and 5. However, the results from the damage vector method show that the damage is almost throughout the entire tower. Even the nodes affected by the simulated damage are in the list of detected damaged nodes, the number of false alarms is too large. As a result, it is very difficult to conclude the damaged location by using the damage vector method with the system equivalent reduction expansion process. Note that the Bayesian damage detection method proposed in this paper can narrow down the damage precisely without false alarms in Damage case 1.

Based on the formulation, the damage vector method requires an accurate finite element model of the target structure. Therefore, model updating is unavoidable for the success of the damage vector method. In addition, mode shape expansion or model reduction is unavoidable. This introduces significant errors to the results of damage detection by using the damage vector method.

4. Conclusions

A damage detection method following Bayesian model updating is proposed. The PDF of uncertain model parameters conditional on a given model class and a given set of measurements was derived. Unlike the deterministic method, measurement from all data sets can be fully utilized without relying only on the mean values of the measured modal parameters. Since natural frequencies and mode shapes of different modes have different level of measurement noise, different weighting factors should be assigned to them in the model updating formulation. By applying Bayesian model updating method, these weighting factors can be calculated through a theoretically rigorous way based on the uncertainties of the measurement. To verify the proposed method, a scale model of a transmission tower was built. Impact hammer tests were carried out on the undamaged structure and two damage cases with limited number of measured DOFs under a multiple setup arrangement. Modal identification on the measured time-domain data was carried out. The identified modal parameters from the undamaged and damaged structures are employed to update the computer model of the target structures. In order to reduce the number of uncertain model parameters, a substructure scheme is proposed. After the identification of the reference structure, the damage in both damage cases was detected by comparing the model updating results of the undamaged and damaged tower. The results of the experimental verification are very positive showing that the proposed damage detection method is feasible for brace damages of tower structures. In the experimental verification, vibration data of only one column was measured. All the simulated damage in both cases can be successfully detected by using only one model class.

The proposed method was verified using data collected from impact hammer tests. In the real application of the proposed method, the property owner may not allow researchers to carry out

impact hammer test. This is because the required magnitude of impact force has to be very large to ensure an appropriate signal to noise ratio, and such a large impact force may damage the structure. It is suggested adopting ambient vibration test to collect vibration data for the purpose of damage detection in real application of the proposed method (Au 2011a; Au *et al.* 2012; Au and Zhang 2012).

In the impact hammer test, the measurement was divided into two setups due to the limited number of accelerometers available. Only one reference was employed (at 45° between the positive x and y directions) for assembling the mode shapes from the two setups. The quality of vibration measurement from this reference sensor is essential for the identification of the torsional modes (with vibration in both x and y directions). For the implementation of the proposed methodology in real situation, it is strongly recommended to install more than one reference sensor along different directions, and the mode shapes can be assembled based on the least square method (Au 2011b) to enhance the robustness of the experimental setup and increase the accuracy of the identified modal parameters.

Acknowledgments

The work described in this paper was fully supported by a grant from the Research Grants Council of the Hong Kong Special Administrative Region, China (Project No. GRF 9041770 CityU 114712).

References

- Au, S.K. (2011a), "Fast Bayesian FFT method for ambient modal identification with separated modes", *J. Eng. Mech.*, ASCE, **137**(3), 214-226.
- Au, S.K. (2011b), "Assembling mode shapes by least squares", *Mech. Syst. Sig. Proc.*, **25**(1), 163-179.
- Au, S.K., Ni, Y.C., Zhang, F.L. and Lam, H.F. (2012), "Full-scale dynamic testing and modal identification of a coupled floor slab system", *Eng. Struct.*, **37**, 167-178.
- Au, S.K. and Zhang, F.L. (2012), "Ambient modal identification of a primary-secondary structure using fast Bayesian FFT approach", *Mech. Syst. Signal Pr.*, **28**, 280-296.
- Beck, J.L. (1978), "Determining models of structures from earthquake records", *Earthquake Engineering Research Laboratory*, California Institute of Technology, Pasadena.
- Beck, J.L. and Katafygiotis, L.S. (1998), "Updating models and their uncertainties. I: Bayesian statistical framework", *J. Eng. Mech.*, ASCE, **124**(4), 455-461.
- Burdekin, F.M. (1993), "Nondestructive testing of welded structural steelwork", *Proc. Inst. Civ. Eng. Struct.*, **99**(1), 89-95.
- ChinaFotoPress/Getty Images AsiaPac (2011), *Eight Dead in Sichuan Transmission Tower Collapse*, <http://www.zimbio.com/pictures/2FVBZhPqCwD/Eight+Dead+Sichuan+Transmission+Tower+Collapse/hOm95DMn5qb>.
- Magix (2008), *Energy deregulation forces wide scale distributed energy*, <http://mgx.com/blogs/2008/03/30/energy-deregulation-forces-wide-scale-distributed-energy/>.
- Katafygiotis, L.S. and Beck, J.L. (1998), "Updating models and their uncertainties. II: Model identifiability", *J. Eng. Mech.*, ASCE, **124**(4), 463-467.
- Lam, H.F., Katafygiotis, L.S. and Mickleborough, N.C. (2004), "Application of a statistical model updating approach on Phase I of the IASC-ASCE structural health monitoring benchmark study", *J. Eng. Mech.*, ASCE, **130**(1), 34-48.

- Lam, H.F., Ng, C.T. and Leung, A.Y.T. (2008), "Multicrack detection on semirigidly connected beams utilizing dynamic data", *J. Eng. Mech.*, ASCE, **134**(1), 90-99.
- Lam, H.F. and Ng, C.T. (2008), "The selection of pattern features for structural damage detection using an extended Bayesian ANN algorithm", *Eng. Struct.*, **30**(10), 2762-2770.
- Lam, H.F. and Yin, T. (2011), "Dynamic reduction-based structural damage detection of transmission towers: Practical issues and experimental verification", *Eng. Struct.*, **33**(5), 1459-1478.
- Li, X.Y. and Law, S.S. (2010), "Matrix of covariance of covariance of acceleration responses for damage detection from ambient vibration measurements", *Mech. Syst. Signal Pr.*, **24**(4), 945-956.
- Kassimali, A. (2011), *Matrix analysis of structures*, Cengage Learning.
- Kim, J.H., Jeon, H.S. and Lee, C.W. (1992), "Application of the modal assurance criteria for detecting and locating structural faults", *Proceedings of the 10th International Modal Analysis Conference*, SEM Society for Experimental Mechanics Inc.
- O'Callahan, J., Avitabile, P. and Riemer, R. (1989), "System equivalent reduction expansion process (SEREP)", *Proceedings of the 7th international modal analysis conference*, Schnectady, Union College, NY, **1**, 29-37.
- Papadimitriou, C. and Papadioti, D.C. (2013), "Component mode synthesis techniques for finite element model updating", *Comput. Struct.*, **126**, 15-28.
- Popovics, J.S. and Rose, J.L. (1994), "A survey of developments in ultrasonic NDE of concrete", *Transactions on Ferroelectrics and Freq. Control*, IEEE, **44**(1), 140-143.
- Vanik, M.W., Beck, J.L. and Au, S.K. (2000), "Bayesian probabilistic approach to structural health monitoring", *J. Eng. Mech.*, ASCE, **126**(7), 738-745.
- Yin, T., Lam, H.F., Chow, H.M. and Zhu, H.P. (2009), "Dynamic reduction-based structural damage detection of transmission tower utilizing ambient vibration data", *Eng. Struct.*, **31**(9), 2009-2019.
- Yaglom, A.M. (1987), *Correlation theory of stationary and related random functions*, Springer-Verlag, Berlin, Germany.
- Yang, J.N., Lei, Y., Lin, S. and Huang, N. (2004), "Hilbert-Huang based approach for structural damage detection", *J. Eng. Mech.*, **130**(1), 85-95.
- Yuen, K.V., Katafygiotis, L.S. and Beck, J.L. (2002), "Spectral density estimation of stochastic vector processes", *Prob. Eng. Mech.*, **17**(3), 265-272.
- Zhong, S.C. and Oyadiji, S.O. (2011), "Detection of cracks in simply-supported beams by continuous wavelet transform of reconstructed modal data", *Comput. Struct.*, **89**(1-2), 127-148.
- Zimmerman, D.C. and Kaouk, M. (1994), "Structural damage detection using a minimum rank update theory", *J. Vib. Acoust.*, **116**, 222-231.